Since January 2020 Elsevier has created a COVID-19 resource centre with free information in English and Mandarin on the novel coronavirus COVID-19. The COVID-19 resource centre is hosted on Elsevier Connect, the company's public news and information website.

Journal of Infection and Public Health 15 (2022) 1180–1191

Contents lists available at ScienceDirect

Journal of Infection and Public Health

journal homepage: www.elsevier.com/locate/jiph

Repurposing of potential antiviral drugs against RNA-dependent RNA polymerase of SARS-CoV-2 by computational approach

Sivakumar Gangadharan [a], Jenifer Mallavarpu Ambrose [b], Anusha Rajajagadeesan [c], Malathi Kullappan [b], Shankargouda Patil [d,e,*], Sri Harshini Gandhamaneni [f], Vishnu Priya Veeraraghavan [e,**], Aruna Kumari Nakkella [g], Alok Agarwal [h], Selvaraj Jayaraman [e], Krishna Mohan Surapaneni [i,**]

[a] Department of Chemistry, Panimalar Engineering College, Varadharajapuram, Poonamallee, Chennai 600123, Tamil Nadu, India
[b] Department of Research, Panimalar Medical College Hospital & Research Institute, Varadharajapuram, Chennai 600123, Tamil Nadu, India
[c] Department of Biochemistry, Panimalar Medical College Hospital & Research Institute, Varadharajapuram, Chennai 600123, Tamil Nadu, India
[d] College of Dental Medicine, Roseman University of Health Sciences, South Jordan, UTAH-84095, USA
[e] Centre of Molecular Medicine and Diagnostics (COMManD), Saveetha Dental College & Hospitals, Saveetha Institute of Medical and Technical Sciences, Saveetha University, Chennai 600077, India
[f] Department of General Medicine, Panimalar Medical College Hospital & Research Institute, Varadharajapuram, Chennai 600123, Tamil Nadu, India
[g] Department of Engineering Chemistry, Dr B R Ambedkar University, Etcherla, Srikakulam 532410, Andhra Pradesh, India
[h] Department of Chemistry, Chinmaya Degree College, BHEL, Haridwar 249403, Uttarakhand, India
[i] Departments of Biochemistry, Molecular Virology, Research, Clinical Skills & Simulation, Panimalar Medical College Hospital & Research Institute, Varadharajapuram, Poonamallee, Chennai 600123, Tamil Nadu, India

ARTICLE INFO

Article history:
Received 10 August 2022
Received in revised form 16 September 2022
Accepted 20 September 2022

Keywords:
Drug repurposing
Antiviral drugs
COVID-19
SARS-CoV-2
RNA-dependent RNA polymerase
RdRp inhibitors
In silico screening
Molecular docking

ABSTRACT

The high incidences of COVID-19 cases are believed to be associated with high transmissibility rates, which emphasizes the need for the discovery of evidence-based antiviral therapies for curing the disease. The rationale of repurposing existing classes of antiviral small molecule therapeutics against SARS-CoV-2 infection has been expected to accelerate the tedious and expensive drug development process. While Remdesivir has been recently approved to be the first treatment option for specific groups of COVID-19 patients, combinatory therapy with potential antiviral drugs may be necessary to enhance the efficacy in different populations. Hence, a comprehensive list of investigational antimicrobial drug compounds such as Favipiravir, Fidaxomicin, Galidesivir, GC376, Ribavirin, Rifabutin, and Umifenovir were computationally evaluated in this study. We performed *in silico* docking and molecular dynamics simulation on the selected small molecules against RNA-dependent RNA polymerase, which is one of the key target proteins of SARS-CoV-2, using AutoDock and GROMACS. Interestingly, our results revealed that the macrocyclic antibiotic, Fidaxomicin, possesses the highest binding affinity with the lowest energy value of −8.97 kcal/mol binding to the same active sites of RdRp. GC376, Rifabutin, Umifenovir and Remdesivir were identified as the next best compounds. Therefore, the above-mentioned compounds could be considered good leads for further preclinical and clinical experimentations as potentially efficient antiviral inhibitors for combination therapies against SARS-CoV-2.

* Correspondence to: College of Dental Medicine, Roseman University of Health Sciences, South Jordan, UTAH-84095, (S.P.) USA.
** Corresponding authors.
E-mail addresses: gsivakumarchemistry@yahoo.com (S. Gangadharan), jenifer.research@pmchri.ac.in (J.M. Ambrose), maya.anusha@gmail.com (A. Rajajagadeesan), malathi.research@pmchri.ac.in (M. Kullappan), dr.ravipatil@gmail.com (S. Patil), sriharshini555@gmail.com (S.H. Gandhamaneni), drvishnupriyav@gmail.com (V.P. Veeraraghavan), drsidvi@gmail.com (A.K. Nakkella), agarwalalok547@gmail.com (A. Agarwal), selarajj.sdc@saveetha.com (S. Jayaraman), krishnamohan.surapaneni@gmail.com, krishnamohan.surapaneni@gmail.com (K.M. Surapaneni).

https://doi.org/10.1016/j.jiph.2022.09.007

Introduction

The COVID-19 pandemic has caused unprecedented medical emergencies all across the globe, which demands the rapid discovery of efficacious and deployable drugs against SARS-CoV-2 virus [1,2]. As of Oct 2020, US FDA has approved the nucleoside antiviral drug, Remdesivir (also called Veklury), for treating particular groups (adult and pediatric) of COVID-19 patients, who are of 12 years of age or older and weighing at least 40 kg, requiring hospitalization [3]. Similarly, another ribonucleotide analog, Molnupiravir, has been recently authorized in UK for treating COVID-19 adult patients with restrictions, as it slightly reduced the risk of hospitalization or death as per the results of their phase 3 clinical trial [4]. However, sufficient experimental and clinical evidence to ensure their efficacy and safety in all the patient groups is still lacking. Despite rigorous vaccination drives, several mutant forms of SARS-CoV-2 continue to spread rapidly at a higher rate in several parts of the world [5]. It is anticipated that the evolution of the pathogen could eventually lead to vaccine-mediated disease enhancement, making the prophylactic vaccines less efficacious over time [6,7]. Therefore, a long-term solution for treating the SARS-CoV-2 infected individuals is to develop potential antiviral therapeutics, which could be used as mono or combination therapies. Accumulating evidence suggests that the drug repurposing strategy focuses on screening several FDA-approved drugs through in vitro and in silico approaches [8,9], as it reduces the time and cost involved in the drug discovery process unlike de novo drug discovery or randomized clinical trials [10–12].

SARS-CoV-2 replication involves a few cardinal proteins namely RNA-dependent-RNA polymerase (RdRp), 3-Chymotrypsin-like protease (3CLpro), Papain-like protease (PLpro), and RNA helicase. These non-structural proteins participate in a series of events such as replication, proofreading, polyprotein cleavage, etc [13–18]. Such functional proteins have been widely studied as potential drug targets because various existing antiviral drugs have substantially inhibited the initial viral replication activities, preventing the disease progressing to hyper-inflammatory state [19,20]. Recent research findings have demonstrated that the pathogen primarily uses RdRp enzyme, which has no host homolog, as its replication and transcription machinery to invade the host immune system [21–23]. Besides this, the active site of RdRp has been found to be highly conserved across several organisms [21]. For this reason, RdRp has been identified as one of the most lucrative and ideal drug discovery targets against SARS-CoV and SARS-CoV-2 [22,24]. The RdRp complex consists of 'non-structural protein 12' (NSP12), which is known as a catalytic subunit along with two other subunits called 'non-structural protein subunits 7 and 8' (NSP7 and NSP8) [25]. Inhibition of RdRp encoded as nsp12, in particular, has become the focus of several ongoing drug designing and discovery research against SARS-CoV-2 [26].

For treating several infections caused by RNA-based viruses like Influenza, Hepatitis C, Zika, Ebola, and many coronaviruses, various antiviral drugs that target RdRp and proteases have been already developed [21]. Some of the FDA-approved RdRp inhibitors such as Hydroxychloroquine, Remdesivir, Ribavirin, Favipiravir, Galidesivir, Kaletra, Sofosbuvir, Tenofovir, and Retonavir have been found to be effective against a broad spectrum of RNA viruses including SARS viruses [26–29]. Thus, antiviral drugs such as Remdesivir and Molnupiravir that target RdRp have been proactively tested against SARS-CoV-2 since when the pandemic started [30,31]. As the experimental validations were found to be partially successful, they have been approved for restricted use only for treating COVID-19 patients belonging to specific groups [32–34]. Similarly, several in silico molecular modelling and preclinical studies have also suggested the plausibility of the above mentioned antiviral compounds to control and prevent the replication and transcription of SARS-CoV-2 [35]. However, those studies have reported different compounds as the top ranked compounds against RdRp [21,36–38]. Identifying potential drug candidates that have promising clinical efficacy to combat and cure the disease is the highest priority to keep this public health threat at bay. Therefore, this study attempted to adapt the drug repurposing *in silico* molecular dynamics simulation approach for RdRp by evaluating a comprehensive list of top-ranked antiviral nucleotide antiviral inhibitors, antibiotics, and antiparasitic compounds that are currently being tested in different phases of clinical trials for COVID-19 treatment and those that have been published previously.

Results

In a matured RdRp complex of SARS-CoV-2, nsp7 and nsp8 get activated thereby conferring the processivity to the nsp12 RNA synthesizing activity [25]. Inhibiting this enzyme would not only disrupt the viral replication process but also minimizes any potential risks in host cells [39]. Hence, RdRp plays a pivotal role in the development of novel therapeutic agents [40]. In this study, we hypothesized that the currently available antiviral drugs could possess the inhibitory potential against RdRp of SARS-CoV-2. Instead of screening compounds from databases, we picked RdRp and proteases-specific inhibitory small molecules from recent analytical studies. Here, we evaluated a panel of seventeen ligands including FDA-approved antiviral drugs that demonstrated substantial H-bond and hydrophobic interactions with key amino acid residues of the active site. Prior to docking, the protein receptor was optimized in order to remove any steric hindrances [41]. Fig. 1 illustrates the tertiary structure of the target protein, with their secondary structural elements highlighted separately.

Our docking results of the chosen inhibitory compounds with NSP12 revealed that certain amino acid residues of the protein formed close contacts with a few of the ligands studied, with binding affinities predicted in a range between −4.89 kcal/mol and −8.97 kcal/mo (Table 1).

When we examined the differences between the binding affinities of the selected antiviral drugs, we found that Fidaxomicin bound with RdRp-NSP12 binding cavity at ARG569, LYS577, ALA685, GLY590, and LYS593 with the lowest binding energy value of −8.97 kcal/mol. Notably, the ligand interaction analysis of Fidaxomicin-RdRp-nsp12 complex showed multiple non-covalent intermolecular interactions like hydrogen bond (H-bond),

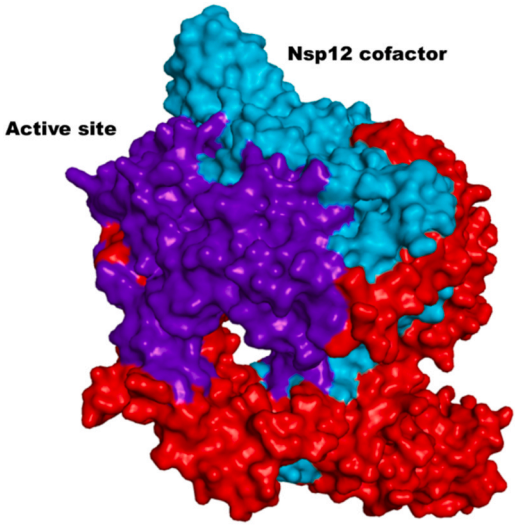

Fig. 1. represents the structure of the RNA-dependent RNA polymerase complex, in which the NSP12 cofactor is highlighted in cyan with the ligand-binding active site indicated in purple.

Table 1
AutoDock docking results of the existing antiviral/antibacterial inhibitors studied.

Compound	PubChem ID	Binding Energy (kcal/mol)
Fidaxomicin	10034073	−8.97
GC376	71481120	−8.6
Rifabutin	135398743	−7.93
Umifenovir	131411	−7.21
Remdesivir	121304016	−6.81
Tenofovir	464205	−6.71
Hydroxychloroquine	3652	−6.59
Galidesivir	10445549	−6.51
Molnupiravir	145996610	−6.49
Chloroquine	2719	−6.42
Rupintrivir	6440352	−6.4
Zanamavir	60855	−6.32
Zidovudine	35370	−6.21
Favipiravir	492405	−6.17
Ribavirin	37542	−6.11
Oseltamivir	65028	−5.52
Sofosbuvir	45375808	−5.28
Kaletra	11979606	−4.89

hydrophobic contacts (Table 2). ARG569, LYS577, ALA685, GLY590, and LYS593 were involved in H-bond formation, while the residues such as ASN497, LYS500, GLN573, LEU576, ILE589, THR591, SER592, LYS593, TRP598, MET601, SER682, ASP684, ALA685, ALA688, TYR689, LEU758, SER759, and GLN815 formed hydrophobic bonds (Fig. 2).

Among the remaining ligands, GC376, Rifabutin, and Umifenovir could bind to the cavity with the binding energy values of −8.6 kcal/mol, −7.93 kcal/mol, and −7.21 kcal/mol respectively. On an average, four H-bonds and nine hydrophobic bonds stabilized the protein-ligand complexes. It is worth-mentioning that LYS545 was involved in building both hydrogen and hydrophobic bonds, which conferred stability to the complex. Likewise, amino acids such as ASN691, ASP760, ASP761, and SER814 formed hydrogen bonds with Rifabutin in addition to ten hydrophobic bonds (Fig. 3).

In the case of the GC376-RdRp-NSP12 complex, six hydrogen bond interactions were observed with LYS545, ARG553, ARG555, THR556, ASP623, and SER682. Besides, nine hydrophobic interactions were observed at ASP452, TYR456, MET542, LYS545, ARG553, ALA554, ALA558, LYS621, and ARG624 (Fig. 4). Unlike other ligands, the receptor-ligand complex made by Umifenovir displayed a single hydrogen bond with TRP617 (1.7 Å) of the protein and eight hydrophobic bonds with ASP618, TYR619, PRO620, LYS621, CYS622, ASP760, ASP761, and LYS798 (Fig. 5). Remdesivir, on the other hand, formed six hydrogen and ten hydrophobic bonds with a higher binding energy value of −6.81 kcal/mol (Fig. 6).

Table 2
Intermolecular H-bond and hydrophobic interactions of top-ranked compounds with RdRp-nsp12 complex.

Compound	H-bond Interactions	Bond Distance (Å)	Hydrophobic Interactions
Fidaxomicin	ARG569	2.1	ASN497, LYS500, GLN573,
	LYS577	1.9	LEU576, ILE589, THR591,
	LYS593	3.4	SER592, LYS593, TRP598,
	GLY590	2.0, 2.4	MET601, SER682, ASP684,
	ALA685	2.8	ALA685, ALA688, TYR689, LEU758, SER759, GLN815
GC376	LYS545	2.6	ASP452, TYR456, MET542,
	ARG553	2.5	LYS545, ARG553, ALA554,
	ARG555	1.7, 1.6, 2.3	ALA558, LYS621, ARG624
	THR556	2.3	
	ASP623	2.0, 2.2	
	SER682	2.6	
Rifabutin	ASN691	2.7	ARG553, TRP 617, ASP618, ALA
	ASP760	2.7	797, TRP800, HIS810, GLU811,
	ASP761	3.2, 3.2, 3.3, 3.2	HIS816, ASP833, ARG836,
	SER814	2.6	
Umifenovir	TRP617	1.7	ASP618, TYR619, PRO620, LYS621, CYS622, ASP760, ASP761, LYS798
Remdesivir	LYS545	1.9, 1.8	ASP452, ARG553, THR556,
	ARG553	2.6	VAL557, LYS621, ASP623,
	ARG555	1.7	ARG624, SER681, ASN691,
	CYS622	1.9	ASP760
	THR680	2.9, 2.2, 2.6	
	SER682	2.8	

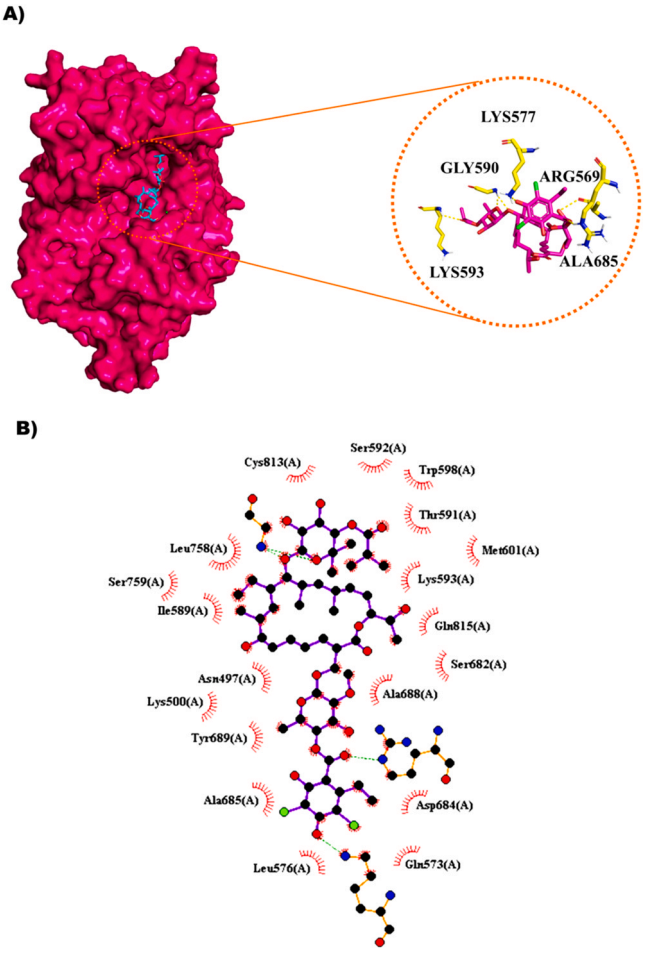

Fig. 2. Representations of protein-ligand complexes from molecular docking. A) 3D diagram of binding conformation of Fidaxomicin with RdRp-nsp12 along with the H-bonds formed in the complex and B) 2D diagram of hydrophobic interactions between Fidaxomicin and RdRp-nsp12 in the docked complex.

Intermolecular H-bond and hydrophobic interactions of top-ranked compounds with RdRp-nsp12 complex.

The interaction energy values of all of the small molecules with the nsp12 amino acid residues that formed stable complexes are presented in Table 2.

The RMSD value of the superimposed structures of the docked RdRp-Remdesivir complex with the available RdRp-Remdesivir complex obtained from PDB (7L1F) was calculated to be 1.957 Å, which verified the reliability of our docking results. Surprisingly, the binding energy of Molnupiravir, which is the first antiviral to be approved in the UK for treating symptomatic COVID-19 cases [31], was comparatively higher (−6.49 kcal/mol) than that of the above-mentioned compounds. Thus, it was ranked ninth among the compounds compared in this study. Although the binding energy of compounds such as GC376, Rifabutin, Umifenovir, Remdesivir was in a similar range according to the previous in silico research studies [36,42], Fidaxomicin gave a slight edge over those compounds by exhibiting the lowest binding energy values.

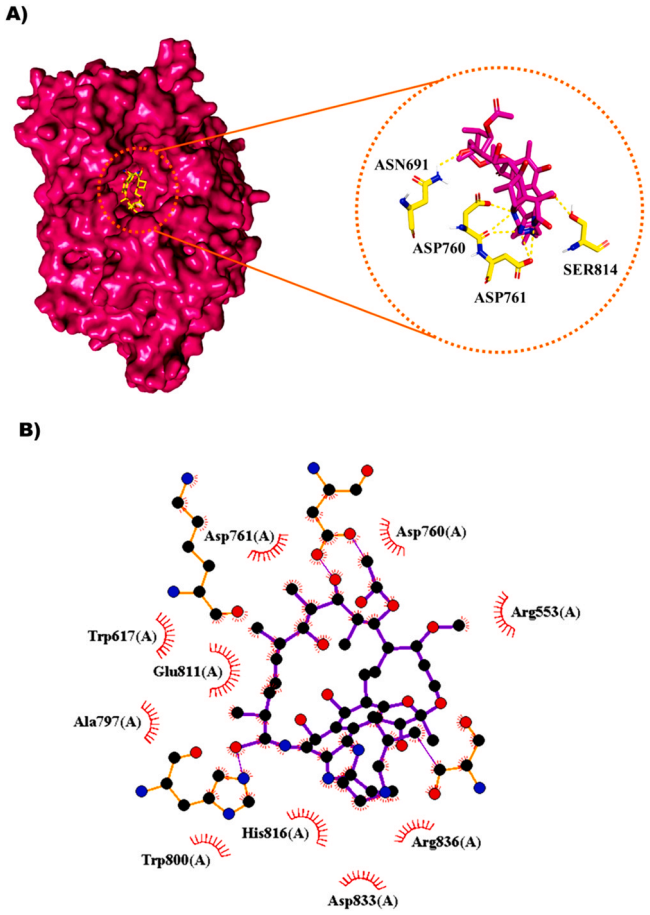

Fig. 3. Representations of protein-ligand complexes from molecular docking. A) 3D diagram of binding conformation of Rifabutin with RdRp-nsp12 along with the H-bonds formed in the complex and B) 2D diagram of hydrophobic interactions between Rifabutin and RdRp-nsp12 in the docked complex.

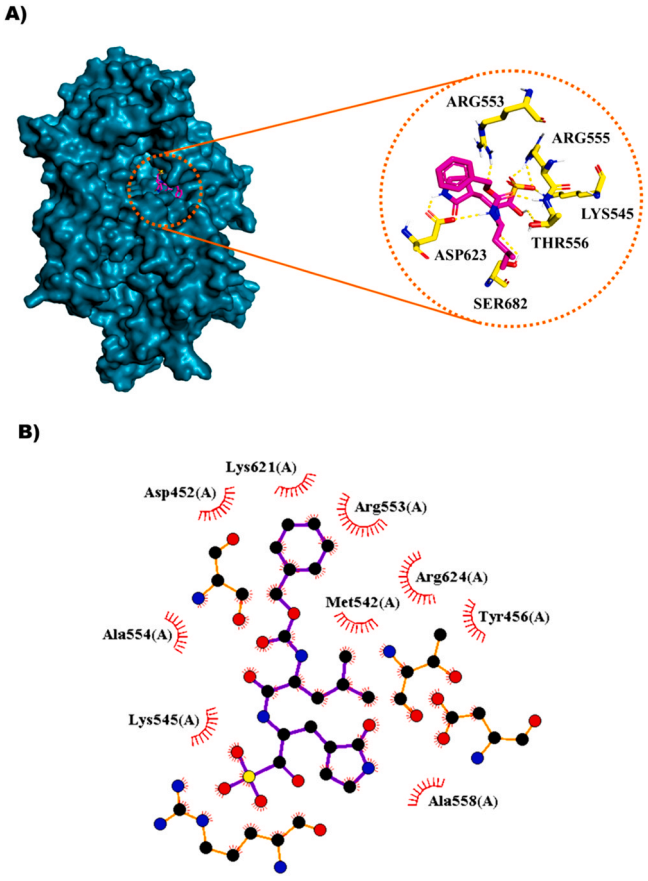

Fig. 4. Representations of protein-ligand complexes from molecular docking. A) 3D diagram of binding conformation of GC376 with RdRp-nsp12 along with the H-bonds formed in the complex and B) 2D diagram of hydrophobic interactions between GC376 and RdRp-nsp12 in the docked complex.

All-atom 100 ns MD simulations were carried out to examine the stability of the docked complexes by MDS package of GROMACS. The RdRp with Fidaxomicin and the standard RdRp inhibitor, Rifabutin were simulated in an explicit solvation system, using their complexes as the starting atomic coordinates. The temperature, energy, density, and other system parameters were continuously monitored, which showed stable molecular dynamics trajectories with slight variations between the two systems at certain time points. Although the root mean square deviation (RMSD) value of the protein backbone with Fidaxomicin and Rifabutin indicated stabilization, the RMSD value of the protein backbone with Rifabutin showed slight deviations during the simulation. While there was low variations in the RMSD values (in the range of 0.15 nm and 0.22 nm) of Fidaxomicin (black), Rifabutin (red) displayed a slight incline in the deviations in their RMSD values beyond 40,000 ps during simulation run, after which it attained stability without any variations (0.3 nm), throughout the simulation run (Fig. 7). These deviation patterns in the protein backbones of the docked complexes were comparable and they depict the thermal stability of Fidaxomicin and the standard RdRp inhibitor, Rifabutin.

Similarly, root mean square fluctuation (RMSF) was calculated, which determines the mobility or flexibility of the residues of a macromolecule with the ligands by looking into the average fluctuation of the position during the simulations. The RMSF values of RdRp in complex with Fidaxomicin and Rifabutin are depicted in Fig. 8, wherein the lower RMSF value (~ 0.2–0.3 nm) of the protein docked with Fidaxomicin (black) confirmed the stability of the protein with minimum motility and flexibility in the docked conformation. In case of RdRp-Rifabutin complex (red), the residues comparatively showed fluctuations in the acceptable range (0.2–0.4 nm) at different time points, when bound to the protein. The difference in the overall fluctuations of the protein suggested that the inhibitory potential of Fidaxomicin was better than Rifabutin against RdRp of SARS-CoV-2. Although the overall difference in the binding nature of the respective ligands was indicated by slightly varying RMSF values, they were in the acceptable range (0.1 nm and 0.4 nm), it did not influence the protein structure and dynamics.

Furthermore, the overall compactness of the polymerase structure in the protein-ligand complex was determined by radii of gyration (Rg) for each of the two complexes studied. Rg values of the RNA-dependent RNA polymerase complexed with the macrocyclic antibiotic, Fidaxomicin and a standard RdRp inhibitor, Rifabutin were ~2.85 nm and ~2.9 nm respectively (Fig. 9). It was revealed that the macromolecular structure became significantly compact when bound to Fidaxomicin (black), as pointed out by the lowest Rg value.

In addition, the total solution accessible surface area (SASA) of RdRp with Fidaxomicin and Rifabutin at 100,000 ps time were calculated as depicted in Fig. 10. Among the two complexes, RdRp with Fidaxomicin (black) exhibited lowest SASA (between 430 and 435 nm^2), like Rg. Thus, the polymerase could contact more solvent molecules, resulting in more flexibility of forming H-bonds during complex formation.

Finally, RdRp with Fidaxomicin exhibited the highest receptor-ligand affinity according to the molecular mechanism Poisson-Boltzmann surface area (MMPBSA) results obtained in our study. The binding free energy value was computed from the MD simulation trajectories. The Gibbs free energy (ΔG_{bind}) of the lead Fidaxomicin

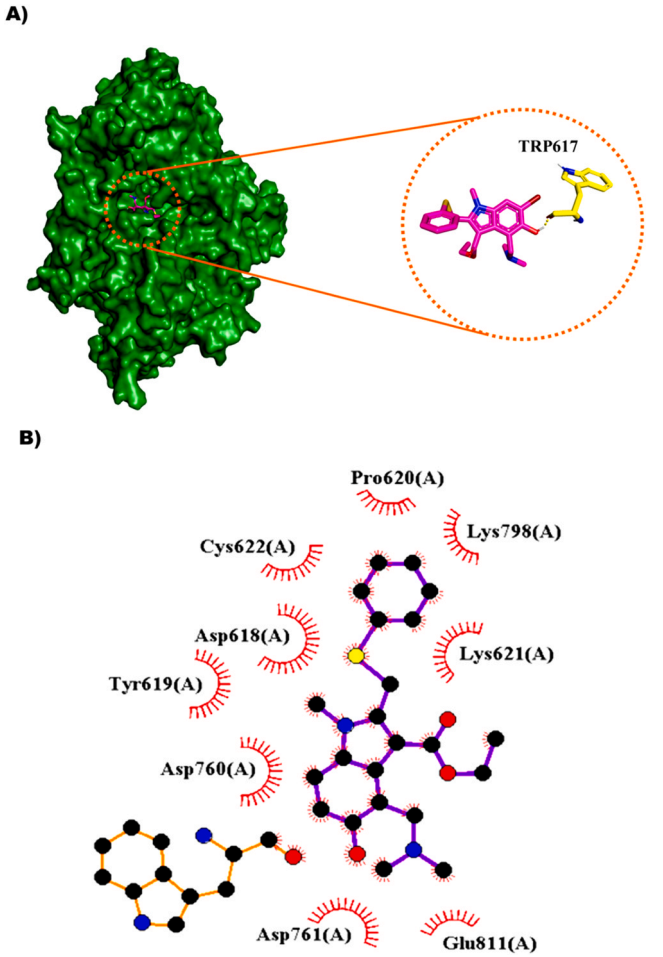

Fig. 5. Representations of protein-ligand complexes from molecular docking. A) 3D diagram of binding conformation of Umifenovir with RdRp-nsp12 along with the H-bonds formed in the complex and B) 2D diagram of hydrophobic interactions between Umifenovir and RdRp-nsp12 in the docked complex.

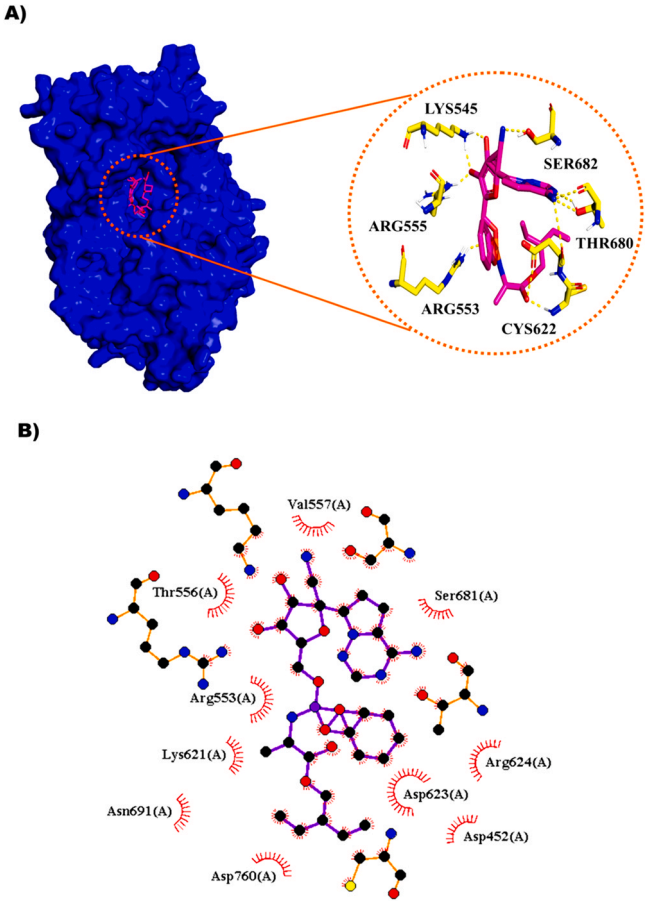

Fig. 6. Representations of protein-ligand complexes from molecular docking. A) 3D diagram of binding conformation of Remdesivir with RdRp-nsp12 along with the H-bonds formed in the complex and B) 2D diagram of hydrophobic interactions occurred between Remdesivir and RdRp-nsp12 in the docked complex.

and Rifabutin-RdRp bound complexes was derived using the equation given as follows:

$$\Delta G_{bind} = G_{complex} - (G_{protein} + G_{ligand})$$

where, $G_{complex}$ represents the energy of the antibiotic Fidaxomicin/RdRp standard inhibitor, Rifabutin, bound protein complex, and $G_{protein}$ and G_{ligand} indicate the individual protein and ligand energy values in the solvated environment, respectively. Further, the thermodynamics parameters of the complex such as van der Waals, electrostatic, polar solvation energies, and SASA were calculated, which are provided in Table 3**.** The cumulative sum of the above-mentioned energies is calculated as the free binding energy. The binding free energy estimated for Fidaxomicin was observed to be the lowest (−334.2 ± 16.7 kj/mol), which remarkably contributed to the molecular interaction between the ligand molecule and RdRp.

The druglikeness prediction of the top five compounds showed that Fidaxomicin had 3 Lipinski violations, while GC376, Rifabutin, and Umifenovir less than 3 violations (Table 4).

ADMET-based parameters of the top five-ranked ligands, when evaluated showed that Fidaxomicin, GC376, Rifabutin, and Umifenovira fulfilled all the criteria, showing to be druggable and safe candidates (Table 5).

It is well documented that the genome of Coronaviruses is the largest among the known RNA viruses, which require an RNA synthesis complex with the fidelity to faithfully replicate their RNA

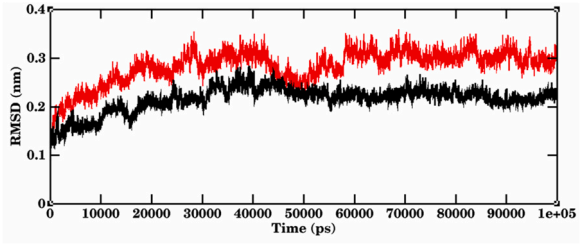

Fig. 7. Representation of MD simulation trajectory RMSD plot of the protein bound to the ligands. The RMSD of RdRp with Fidaxomicin complex (black) and RdRp with Rifabutin complex (red) were obtained during 100,000 ps simulation.

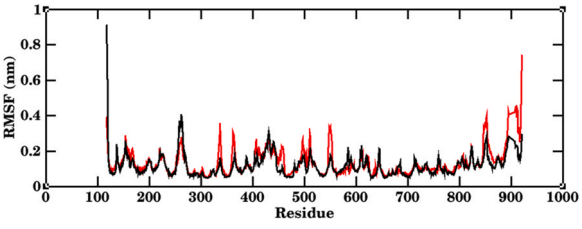

Fig. 8. Representation of MD simulation trajectory RMSF plot of the protein bound to the ligands. The RMSF of RdRp with Fidaxomicin complex (black) and RdRp with Rifabutin complex (red) were obtained during 100,000 ps simulation.

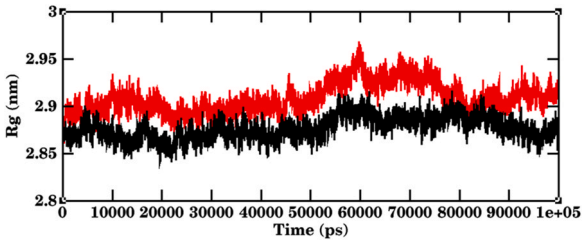

Fig. 9. Representation of MD simulation trajectory Rg plot of the protein bound to the ligands. The Rg of RdRp with Fidaxomicin complex (black) and RdRp with Rifabutin complex (red) were obtained during 100,000 ps simulation.

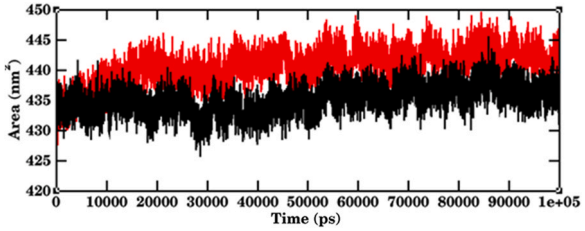

Fig. 10. Representation of MD simulation trajectory SASA plot of the protein bound to the ligands. The SASA of RdRp with Fidaxomicin complex (black) and RdRp with Rifabutin complex (red) were obtained during 100,000 ps simulation.

[43]. In the recent years, various research groups have demonstrated the feasibility to block RdRp with various extents to expedite the development of potential drugs against RNA viruses like HCV2 [44], H1N11 [45], HIV3 [46], SARS [47], MERS [47], Chikungunya [48], Dengue [49], and Zika [50]. Fidaxomicin is a bactericidal macrocyclic lactone antibiotic that has been previously known to mediate its potent bactericidal action as it inhibits the bacterial RNA synthase, thereby deranging the transcription in Clostridium difficile [51]. Latest experimental reports have identified that Fidaxomicin could significantly suppress the viral replicase activity in Zika virus infected cells by blocking the complex formation between RNA polymerase and its open promoter with higher specificity [52]. According to their in vitro and in vivo experiments, Fidaxomicin was effective against a wide variety of Zika virus cell lines by prominently suppressing the infection and remarkably improving the survival of infected mice [50]. Another experimental study, which evaluated the antiviral inhibitors against SARS-CoV-2, has confirmed that GC376 in combination with the nucleoside analog, Remdesivir, completely inhibited the replication mechanism in SARS-CoV-2 infected cells [53]. Similarly, Rifabutin, which is a first-line anti-tuberculosis drug, has demonstrated remarkable clinical efficacy by inhibiting RNA polymerase and has been used as an alternative drug among HIV patients co-infected with tuberculosis as reported by a clinical trial experimental study [54]. Likewise, the findings of another experimental study have suggested that Umifenovir and its analog to be promising antiviral agents as it showed direct inhibitory effect on the SARS-infected cells by disrupting the early viral replication [55].

As observed in other RNA virus, the highly conserved nature of RdRp, whose structural motifs like 315-GDD-317 and the metal catalytic site within it, is considered to promote the incoming nucleotide triphosphate (NTPs) for RNA replication and elongation [56]. Although some of the compounds studied here have been previously

Table 3
Summary of binding free energy and other interaction energies.

Complex	$\Delta E_{binding}$ (kj/mol)	$\Delta E_{electrostatic}$ (kj/mol)	$\Delta E_{van\ der\ Waal}$ (kj/mol)	$\Delta E_{polar\ solvation}$ (kj/mol)	ΔE_{SASA} (kj/mol)
Fidaxomicin	−334.2 ± 16.7	−124.8 ± 13.9	−292.8 ± 21.1	113.3 ± 17.7	−29.9 ± 1.4
Rifabutin	−326.5 ± 13.6	−119.1 ± 12.7	−288.2 ± 22.3	105.9 ± 16.6	−25.1 ± 2.1

Table 4
Prediction of Druglikeness for the top five ligands.

Sl. No.	Ligand	MW (< 500 Da)	HBD (< 5)	HBA (< 10)	Log P (< 5)	A (40–130)	No. of Violations
1	Fidaxomicin	1058.04	7	18	5.67	268.58	3
2	GC376	485.6	5	8	0.99	122.68	1
3	Rifabutin	847.00	5	14	5.11	244.97	2
4	Umifenovir	477.41	1	4	3.79	122.69	0
5	Remdesivir	602.58	4	12	3.24	150.43	2

MW Molecular weight, HBD No of hydrogen bond donors, HBA No of hydrogen bond acceptors, Log P the logarithm of octonal/water partition coefficient, A Molar refractivity.

Table 5
Evaluation of ADMET properties for the top five compounds.

Models	Fidaxomicin	GC376	Rifabutin	Umifenovir	Remdesivir
Absorption					
BBB	BBB-	BBB-	BBB-	BBB-	BBB-
HIA	HIA+	HIA+	HIA+	HIA+	HIA+
Permeability					
PGS	Substrate	Substrate	Substrate	NS	Substrate
Metabolism					
CYP450 1A2 Inhibitor	NI	NI	NI	NI	NI
CYP450 2C9 Inhibitor	NI	NI	NI	Inhibitor	NI
CYP450 2D6 Inhibitor	NI	NI	NI	Inhibitor	NI
CYP450 2C19 Inhibitor	NI	NI	NI	Inhibitor	NI
CYP450 3A4 Inhibitor	NI	NI	NI	Inhibitor	Inhibitor
CYP Inhibitory Promiscuity	Low	Low	Low	High	High
Toxicity					
AMES Toxicity	NAT	NAT	AMES toxic	NAT	NAT
Carcinogens	NC	NC	NC	NC	NC

BBB blood-brain barrier, HIA human intestinal absorption, PGS P-glycoprotein substrate, PGI P-glycoprotein inhibitor, ROCT renal organic cation transporter, NS non-substrate, NI non-inhibitor, NAT non-AMES toxic, NC non-carcinogenic.

reported as binding to the RdRp active site and possibly inhibiting its activity [21,57], the *in silico* docking and dynamics simulations executed for the selected compounds in this study have predicted that Fidaxomicin, GC376, Rifabutin, Umifenovir, and Remdesivir to be promising drug candidates. However, these non-nucleoside ligands were noticed to bepredominantly bound in the finger domain, and in certain parts of the palm and thumb domains of the RdRp structure, rather than interacting at the conserved catalytic site of the target protein. Instead, all the four compounds were [43,58]. The amino acid residues, which interacted with the top-ranked ligands, were in agreement with the previous SARS-CoV-2 research reports [58]. From the molecular docking and simulation results obtained, we observed that amino acid residues such as ASP452, LYS500, LYS545, ARG553, ARG555, THR556, LYS621, ASP623, SER682, ASN691, and ASP760 were commonly involved in the molecular interactions forming hydrophobic bonds. Most of these residues spanning different conserved motifs like motifs B, C, E, F, G, and ligand-binding motif, showed favorable binding with significantly lower free energy values as published by the recent study reports [58,59]. Moreover, the lowest binding free energy (maximum negative binding energy) of Fidaxomicin confirmed its inhibitory potential. Thus, the docking interactions of the aforementioned inhibitors with the NSP12 domains inferred that the interacting amino acids lie within the active site of polymerase. The clinical significance of these observations needs further preclinical and clinical investigations to confirm the antiviral inhibitory potential of the identified ligands as predicted in this study.

Besides the hydrogen and hydrophobic bond formation mentioned above, the minimum structural deviations showed by Fidaxomicin and Rifabutin in the dynamics simulation environment at a 100 ns timescale have reinforced the highest binding affinity exhibited by the protein-ligand complexes. The polar surface area that is exposed by the target receptor confers stable binding site to RdRp [41]. Similarly, the lowest Rg scores that were estimated between 2.85 nm and 2.95 nm for the selected systems inferred higher compactness of the folded protein and thus, confirming the greater structural stability of the protein-ligand complexes. Specifically, the data showed that RdRp-Fidaxomicin complex was more compact and rigid than RdRp-Rifabutin complex. However, both the systems were observed to converge well. Similar findings reported by previous studies were in agreement with the observations made in the present study [59–61]. Similarly, an average surface area of 430 nm^2 was observed for Fidaxomicin and 437.5 nm^2 for Rifabutin through the 10,000 ps simulation period. Although the SASA value of both the ligands was noticed to be as high as 445 nm^2 at the beginning and minimally fluctuated until 40,000 ps, the lowest SASA value was obtained for the ligands after 90,000 ps. This suggested that the major part of the ligands were buried into the protein towards the end of the simulation, rather than interacting with the aqueous environment. Thus, SASA profiles signified the conformational changes that might have happened during the protein-ligand interactions. The results obtained were in agreement with the previous studies [62,63]. According to the MM-PBSA free energy calculated between RdRp and the ligands, the binding free energy (ΔG_{bind}) of RdRp-Fidaxomicin (−334.2 ± 16.7 kj/mol) was stronger than that of RdRp-Rifabutin (−326.5 ± 13.6 kj/mol), which was in line with the results of docking and MD simulation. In both the systems, we noticed that the major contribution to the total bindind free energy was from van der Waals interaction ($\mathbf{\Delta E_{van\ der\ Waal}}$). The electrostatic interaction ($\mathbf{\Delta E_{electrostatic}}$) was found to be almost neutralized by the polar desolvation energy ($\mathbf{\Delta E_{polar\ solvation}}$) and hence the net electrostatic interactions was unfavourable to the binding affinities. Recent simulation studies on RdRp have reported similar interaction pattern with major van der Waal interactions [63,64]. The binding analysis of RdRp-Fidaxomicin revealed the total binding free energy contributed by individual amino acids such as ARG569, LYS500, LEU576, LYS577, LYS593, MET601, SER759, and ALA797 was remarkable during the complex formation (Fig. 11). Similarly, RdRp-Rifabutin binding involved amino acids such as THR591, LYS593, MET601, LYS577, TYR689, ASP760, SER814 and ARG836, which significantly contributed to the total binding free energy of the complex (Fig. 12). Previous docking and simulation studies of RdRp with various inhibitors including natural compounds have showed similar amino acids that are in agreement with the findings of the present study [63,64].

Overall, the purpose of this study was to evaluate the binding affinity of a set of seventeen known antimicrobial compounds that participate in various levels of clinical trials for COVID-19 worldwide. RNA-dependent RNA polymerase, being one of the principal components of the viral replication machinery, was chosen for this study. Our results corroboratively revealed that the antibiotic, Fidaxomicin, exhibited favorable interaction with the highest binding affinity to RdRp that plays a pivotal role in the regulation of viral replication, transcription, and viral maturation mechanisms in host cells. In addition, compounds such as GC376, Rifabutin, Umifenovir, and Remdesivir showed higher binding activity towards the target macromolecule, over other compounds investigated. Although Fidaxomicin has previously demonstrated its inhibitory effect against flaviviruses like Zika and Dengue, our in silico analysis has provided a valuable clue on its efficacy, which needs to be assessed further with respect to SARS-CoV-2. Of all the compounds, Fidaxomicin and Rifabutin exhibited stable conformations with the RdRp protein with highest binding energy and favourable binding interactions during the 100, 000 ps MD simulation in the present study. Hence, Fidaxomicin and Rifabutin could be effective against RdRp of SARS-CoV-2. Therefore, experimental studies could be initiated or redirected to evaluate the clinical endpoints of these potential drug candidates as viable therapeutic agents against SARS-CoV-2 and its emerging variants like Omicron.

Materials and methods

Selection and preparation of the macromolecule and ligands

As mentioned above, this molecular modeling study selected the SARS-CoV-2 RNA-dependent RNA polymerase protein that plays a crucial role in viral propagation. RdRp is a complex made of NSP12 and its cofactors (NSP7 and NSP8) that offers to be a potential target for several antiviral inhibitors [40]. We retrieved the recently elucidated three dimensional structure of SARS-CoV-2 RdRp nsp12 that was bound to nsp7 and nsp8 cofactors, (6NUR) from the PDB database. By using the AutoDocktools (ADT), the crystal structure of the selected macromolecule was optimized by removing water molecules, adding hydrogen atoms, minimizing energy, and performing 3D protonation to facilitate accurate docking. Similarly, after conducting an extensive literature survey on the antiviral drugs that target and inhibit the activity of RdRp, a set of seventeen antiviral compounds were selected for the study. Antiviral inhibitors such as Chloroquine, Favipiravir, Fidaxomicin, Galidesivir, GC376, Hydroxychloroquine, Kaletra, Molnupiravir, Oseltamivir, Remdesivir, Ribavirin, Rifabutin, Rupintrivir, Sofosbuvir, Tenofovir, Umifenovir, Zanamavir, and Zidovudine were evaluated in this study [65,66]. To determine the differences in the inhibitory potential of the ligands chosen, we retrieved the 3D/2D conformers of the compounds as SDF files from the NCBI-PubChem database (Fig. 13). The chemical structures obtained were subsequently converted to PDB format using the Open Babel toolbox.

Molecular docking

We performed molecular docking at the active site present in chain A of the catalytic subunit, nsp12 of RdRp complex. The input

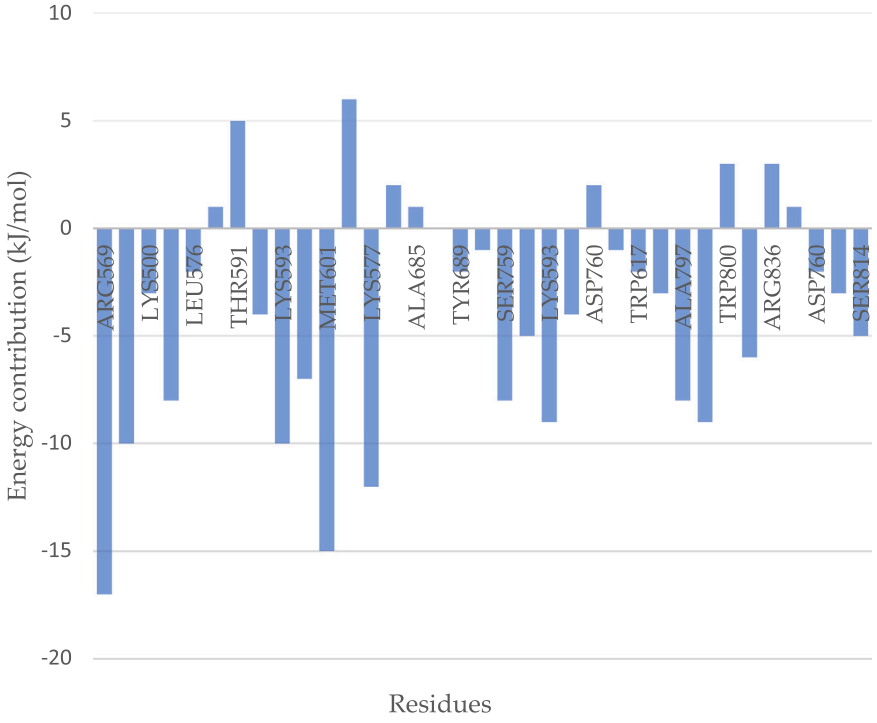

Fig. 11. Per residue contribution plot of RdRp-Fidaxomicin complex.

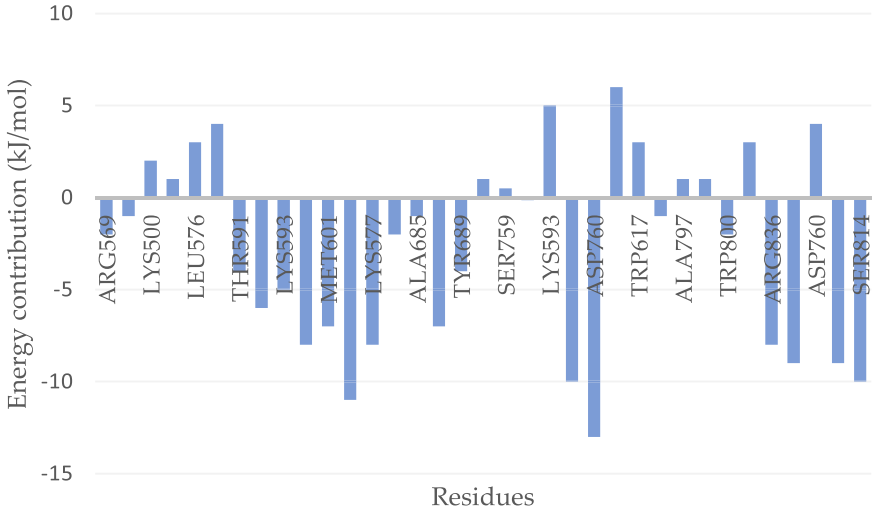

Fig. 12. Per residue contribution plot of RdRp-Rifabutin complex.

files were prepared using AutoDocktool v. 4.2.6. Following the preparation of input files, a grid box was defined in order to confine the binding of ligands in the active site region of the protein. To this aim, previously known ligand-binding interfaces were cataloged to aid in enclosing the box at the centre of the active site. Amino acids such as TYR455, TYR456, THR462, CYS482, TYR483, SER549, THR586, THR591, THR604, TYR619, CYS622, THR680, SER681, SER682, THR686, THR687, TYR689, SER692, CYS697, THR701, SER754, SER681, SER682, THR686, THR687, TYR689, SER692, CYS697, THR701, SER754, SER759, CYS765, SER778, TYR788, SER795, CYS799, THR801, CYS813, SER814, and THR817 were allowed to interact with the chosen ligand set [67]. Accordingly, the protein was enclosed in a grid box of 30 Å × 30 Å × 30 Å, along the X, Y, and Z axes (centred at 114.86 Å, 114.53 Å, 122.91 Å) respectively. Molecular docking was launched by feeding in the preprocessed protein and ligand files, which resulted in ten binding conformations. For each ligand, the conformation with the lowest binding energy was selected as the best pose for further analysis. Subsequently, the docked poses were ranked based on their predicted binding energies. Molecular visualization of the docked complexes was performed using Pymol v. 2.3.

Molecular dynamics simulation

Molecular dynamics simulations for the top ranked compound, Fidaxomicin, and a standard RdRp inhibitor, Rifabutin were carried out using GROMACS version 2019.4 [37], in Ubuntu environment (20.04.1). To begin with, protein structures were converted to gromacs file format and subsequently topology files were generated using CHARMM36 force field. Similarly, the charges and parameters of the ligands were generated by CHARMM General Force Field

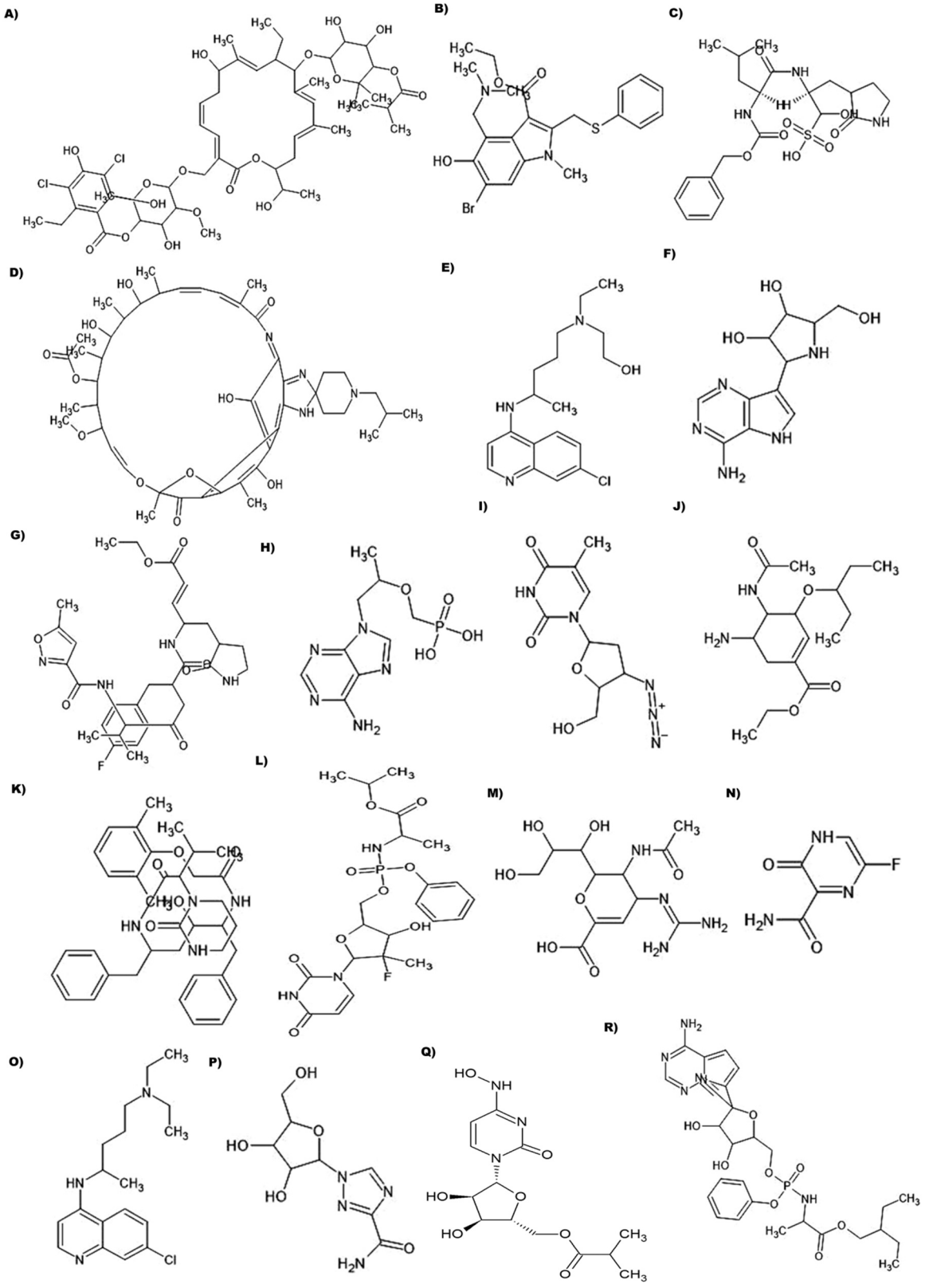

Fig. 13. The chemical structures of the antiviral drug compounds that were selected for the study. A) Fidaxomicin, B) Umifenovir, C) GC376, D), Rifabutin, E), Hydroxychloroquine, F) Galidesivir, G) Rupintrivir, H), Tenofovir, I) Zidovudine, J) Oseltamivir, K) Lopinavir, L) Sofosbuvir, M), Zanamavir, N), Favipiravir, O) Chloroquine, P) Ribavirin, Q) Molnupiravir, and R) Remdesivir.

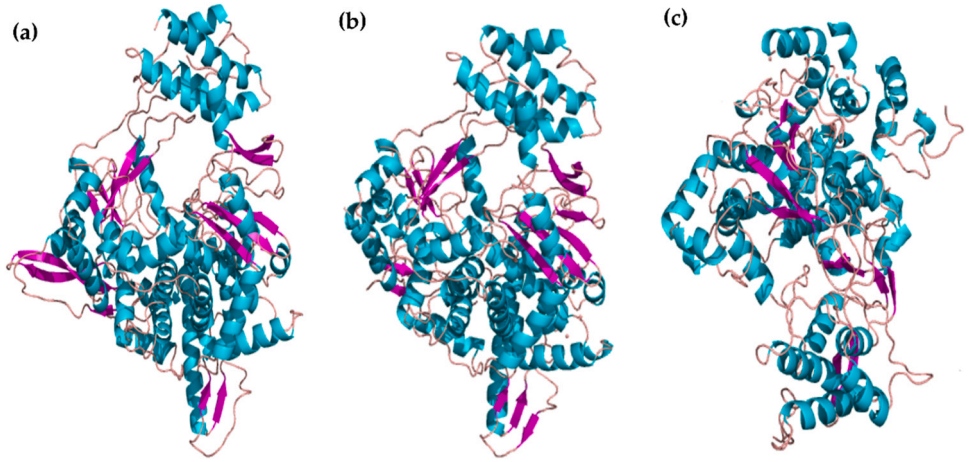

Fig. 14. Conformation of RdRp that was in complex with Rifabutin during MD simulation at a) 0 ns, b) 50 ns, and c) 100 ns timescale.

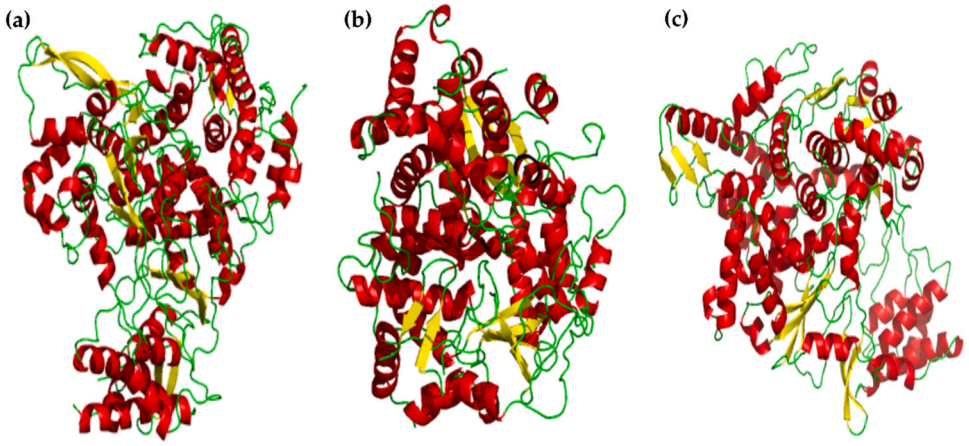

Fig. 15. Conformation of RdRp that was in complex with Rifabutin during MD simulation at a) 0 ns, b) 50 ns, and c) 100 ns timescale.

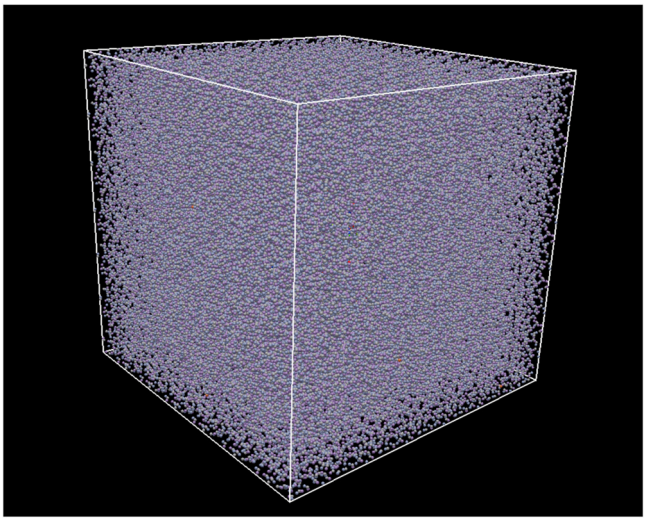

Fig. 16. Snapshots of RdRp-Fidaxomicin and RdRp-Rifabutin complexes during MD simulation.

(CGenFF) version 4.4 webserver. Prepared complex structures were immersed in a dodecahedron solvent box filled with TIP3P water molecules [68]. The dodecahedron box dimensions for periodic boundary conditions were calculated to be 7.748 nm × 8.168 nm × 8.383 nm,. To neutralize the system, we added 12 Na^+ atoms to the solution. The entire system was subjected to energy minimization by steepest descent algorithm and maximum force F_{max} was set not to exceed 1000 kJ/mol.nm. The system was equilibrated by short constraint dynamics under conditions of constant volume, temperature (300 K) and pressure (1 bar) by two consecutive 100 ps simulations with canonical NVT and isobaric NPT ensembles respectively [37]. Thus, the steric clashes between the atoms of proteins, waters, and ions were removed by independently restraining the coordinates of the simulated system, and were thermostat coupled for the entire simulation. MD simulations were run for 100,000 ps with stable temperature and pressure with a time step of 2 fs (Figs. 14–16). All the simulations were carried out using Intel Xeon W-1270, 8 core, and 16 threaded processors. We analyzed the obtained trajectories using GROMACS tools and the RMSD, RMSF, Rg, SASA, and MMPBSA analysis graphs were plotted using Xmgrace.

Druglikeness and ADMET Analysis of potential candidates

Furthermore, the druglikeness and ADMET (absorption, distribution, metabolism, excretion and toxicity) properties of each ligand were comprehensively evaluated using SwissADME respectively.

Conclusion

In conclusion, we have predicted the efficacy of a set of potential antiviral compounds, which are either currently existing antimicrobial drugs or participating in the ongoing clinical trials for SARS-CoV-2. Our in silico assessment corroborated that Fidaxomicin could be efficient clinically in use antibacterial/antiviral drugs, as it effectively attached to the active site of RdRp protein. In addition, GC376, Rifabutin, Umifenovir, and Remdesivir were found to be the next best compounds against the target macromolecule. Therefore, the findings of our drug repurposing approach suggest that the four FDA-approved drugs along with Remdesivir could be potential SARS-CoV-2 antiviral leads in halting the viral replication, which require further preclinical and clinical investigations. Thus, this study could offer a foundation for developing of novel mono/combination therapeutics to the cure the infections caused by SARS-CoV-2 and other emerging RNA viruses.

Funding

This research study received no external funding.

Authors contribution

Conceptualization: SG, JMA and SKM; Methodology: JMA and SKM; Software: JMA, MK and SKM; Validation: SG, JMA, AR, MK, SP, SHG, VPV, AKN, AA, SJ, and SKM; Formal Analysis: JMA, MK and SKM; Investigation: SG, JMA, AR, MK, SP, SHG, VPV, AKN, AA, SJ, and SKM; Resources: SKM; Data Curation: JMA and SKM; Writing – Original draft preparation: JMA and SKM; Writing –Review & Editing: SG, JMA, AR, MK, SP, SHG, VPV, AKN, AA, SJ, and SKM; Visualization: SG, JMA, MK and SKM; Supervision: SKM; Project Administration: SKM; and Funding Acquisition: SP, VPV, and SKM.

Data Availability

The data that supports this study are available upon request from the corresponding author.

Conflicts of interest

The authors declare that there are no conflicts of interests.

Acknowledgments

The authors acknowledge Panimalar Medical College Hospital & Research Institute for providing the docking and simulation resources needed for conducting and publishing this study.

Appendix A. Supporting information

Supplementary data associated with this article can be found in the online version at doi:10.1016/j.jiph.2022.09.007.

References

[1] Prajapat M, Sarma P, Shekhar N, Avti P, Sinha S, Kaur H, et al. Drug targets for corona virus: a systematic review. Indian J Pharmacol 2020;52:56.
[2] Qu YM, Kang EM, Cong HY. Positive result of Sars-Cov-2 in sputum from a cured patient with COVID-19. Travel Med Infect Dis 2020;34:101619.
[3] ⟨https://www.fda.gov/drugs/news-events-human-drugs/fdas-approval-veklury-remdesivir-treatment-covid-19-science-safety-and-effectiveness.⟩.
[4] ⟨https://www.gov.uk/government/publications/nervtag-antiviral-drug-resistance-and-the-use-of-directly-acting-antiviral-drugs-daas-for-covid-19–8-december-2021/nervtag-antiviral-drug-resistance-and-the-use-of-directly-acting-antiviral-drugs-daas-for-covid-19–8-december-2021⟩.
[5] Yang HC, Chen CH, Wang JH, Liao HC, Yang CT, Chen CW, et al. Analysis of genomic distributions of SARS-CoV-2 reveals a dominant strain type with strong allelic associations. Proc Natl Acad Sci USA 2020;117:30679–86.
[6] Zellweger Raphaël M, Anh Wartel T, Marks Florian, Song Manki, Kim Jerome H. Vaccination against SARS-CoV-2 and disease enhancement–knowns and unknowns. Expert Rev Vaccin 2020;19:691–8.
[7] Williams TC, Burgers WA. SARS-CoV-2 evolution and vaccines: cause for concern? Lancet Respir Med 2021;9:333–5.
[8] Guan WJ, Ni ZY, Hu Y, Liang WH, Ou CQ, He JX, et al. Clinical characteristics of coronavirus disease 2019 in China. N Engl J Med 2020;382:1708–20.
[9] Wang M, Cao R, Zhang L, Yang X, Liu J, Xu M, et al. Remdesivir and chloroquine effectively inhibit the recently emerged novel coronavirus (2019-nCoV) in vitro. Cell Res 2020;30:269–71.
[10] Cheng F, Murray JL, Rubin DH. Drug repurposing: new treatments for Zika virus infection? Trends Mol Med 2016;22:919–21.
[11] Cheng F. In silico oncology drug repositioning and polypharmacology. Cancer Bioinforma 2019:243–61.
[12] Zhou Y, Hou Y, Shen J, Huang Y, Martin W, Cheng F. Network-based drug repurposing for novel coronavirus 2019-nCoV/SARS-CoV-2. Cell Discov 2020;6:1–18.
[13] Ibrahim IM, Abdelmalek DH, Elshahat ME, Elfiky AA. COVID-19 spike-host cell receptor GRP78 binding site prediction. J Infect 2020;80:554–62.
[14] Thiel V, Ivanov KA, Putics A, Hertzig T, Schelle B, Bayer S, et al. Mechanisms and enzymes involved in SARS coronavirus genome expression. J Gen Virol 2003;84:2305–15.
[15] Hilgenfeld R. From SARS to MERS: crystallographic studies on coronaviral proteases enable antiviral drug design. FEBS J 2014;281:4085–96.
[16] Agostini ML, Andres EL, Sims AC, Graham RL, Sheahan TP, Lu X, et al. Coronavirus susceptibility to the antiviral remdesivir (GS-5734) is mediated by the viral polymerase and the proofreading exoribonuclease. MBio 2018;9. e00221-18.
[17] Ivanov KA, Thiel V, Dobbe JC, Van Der Meer Y, Snijder EJ, Ziebuhr J. Multiple enzymatic activities associated with severe acute respiratory syndrome coronavirus helicase. J Virol 2004;2004(78):5619–32.
[18] V'kovski P, Kratzel A, Steiner S, Stalder H, Thiel V. Coronavirus biology and replication: implications for SARS-CoV-2. Nat Rev Microbiol 2021;19:155–70.
[19] Sanders JM, Monogue ML, Jodlowski TZ, Cutrell JB. Pharmacologic treatments for coronavirus disease 2019 (COVID-19): a review. Jama 2020;323:1824–36.
[20] Siddiqi HK, Mehra MR. COVID-19 illness in native and immunosuppressed states: A clinical–therapeutic staging proposal. J Heart lung Transplant 2020;39:405.
[21] Elfiky AA. Ribavirin, Remdesivir, Sofosbuvir, Galidesivir, and Tenofovir against SARS-CoV-2 RNA dependent RNA polymerase (RdRp): a molecular docking study. Life Sci 2020;253:117592.
[22] Hillen HS, Kokic G, Farnung L, Dienemann C, Tegunov D, Cramer P. Structure of replicating SARS-CoV-2 polymerase. Nature 2020;584:154–6.
[23] Posthuma CC, Te Velthuis AJ, Snijder EJ. Nidovirus RNA polymerases: complex enzymes handling exceptional RNA genomes. Virus Res 2017;234:58–73.
[24] Snijder EJ, Decroly E, Ziebuhr J. The nonstructural proteins directing coronavirus RNA synthesis and processing. Adv Virus Res 2016;96:59–126.
[25] Subissi L, Posthuma CC, Collet A, Zevenhoven-Dobbe JC, Gorbalenya AE, Decroly E, et al. One severe acute respiratory syndrome coronavirus protein complex integrates processive RNA polymerase and exonuclease activities. Proc Natl Acad Sci USA 2017;111:E3900–9.
[26] Sinha N, Balayla G. Hydroxychloroquine and covid-19. Postgrad Med J 2020;96:550–5.
[27] Li J, McKay KT, Remington JM, Schneebeli ST. A computational study of cooperative binding to multiple SARS-CoV-2 proteins. Sci Rep 2021;2021(11):1–9.
[28] Mitjà O, Clotet B. Use of antiviral drugs to reduce COVID-19 transmission. Lancet Glob Health 2020;8:e639–40.
[29] Yavuz, Serap, Ünal Serhat. Antiviral treatment of COVID-19. Turk J Med Sci 2020;50:611–9.
[30] Elsawah HK, Elsokary MA, Abdallah MS, ElShafie AH. Efficacy and safety of remdesivir in hospitalized Covid-19 patients: systematic review and meta-analysis including network meta-analysis. Rev Med Virol 2021;31:e2187.
[31] ⟨https://www.clinicaltrials.gov/ct2/show/NCT04575597⟩.
[32] Harrison C. Coronavirus puts drug repurposing on the fast track. Nat Biotechnol 2020;38:379–81.
[33] Lung J, Lin YS, Yang YH, Chou YL, Shu LH, Cheng YC, et al. The potential chemical structure of anti-SARS-CoV-2 RNA-dependent RNA polymerase. J Med Virol 2020;92:693–7.
[34] L Zhang, R Zhou, Binding mechanism of remdesivir to SARS-CoV-2 RNA dependent RNA polymerase; 2020.
[35] Wang Y, Li P, Rajpoot S, Saqib U, Yu P, Li Y, et al. Comparative assessment of favipiravir and remdesivir against human coronavirus NL63 in molecular docking and cell culture models. Sci Rep 2021;6(11):1–3.
[36] Parvez MS, Karim MA, Hasan M, Jaman J, Karim Z, Tahsin T, et al. Prediction of potential inhibitors for RNA-dependent RNA polymerase of SARS-CoV-2 using comprehensive drug repurposing and molecular docking approach. Int J Biol Macromol 2020;163:1787–97. Nov 15.
[37] Rafi MO, Bhattacharje G, Al-Khafaji K, Taskin-Tok T, Alfasane MA, Das AK, et al. Combination of QSAR, molecular docking, molecular dynamic simulation and MM-PBSA: analogues of lopinavir and favipiravir as potential drug candidates against COVID-19. J Biomol Struct Dyn 2020;17:1–20.
[38] Ercan S, Çınar E. A molecular docking study of potential inhibitors and repurposed drugs against SARS-CoV-2 main protease enzyme. J Indian Chem Soc 2021;98:100041.
[39] Hasan MK, Kamruzzaman M, Manjur OHB, Mahmud A, Hussain N, Mondal MSA, et al. Structural analogues of existing anti-viral drugs inhibit SARS-CoV-2 RNA

dependent RNA polymerase: a computational hierarchical investigation. Heliyon 2021;7:e06435.
[40] Gao Y, Yan L, Huang Y, Liu F, Zhao Y, Cao L, et al. Structure of the RNA-dependent RNA polymerase from COVID-19 virus. Science 2020;368:779–82.
[41] Qazi S, Das S, Khuntia BK, Sharma V, Sharma S, Sharma G, et al. In silico molecular docking and molecular dynamic simulation analysis of phytochemicals from indian foods as potential inhibitors of SARS-CoV-2 RdRp and 3CLpro. Nat Prod Commun 2020;16. 934578X211031707.
[42] Abdellatiif MH, Ali A, Ali A, Hussien MA. Computational studies by molecular docking of some antiviral drugs with COVID-19 receptors are an approach to medication for COVID-19. Open Chem 2021;19:245–64.
[43] Kirchdoerfer RN, Ward AB. Structure of the SARS-CoV nsp12 polymerase bound to nsp7 and nsp8 co-factors. Nat Commun 2019;10:1–9.
[44] Hofmann WP, Herrmann E, Sarrazin C, Zeuzem S. Ribavirin mode of action in chronic hepatitis C: from clinical use back to molecular mechanisms. Liver Int 2008;28:1332–43.
[45] Lin MI, Su BH, Lee CH, Wang ST, Wu WC, Dangate P, et al. Synthesis and inhibitory effects of novel pyrimido-pyrrolo-quinoxalinedione analogues targeting nucleoproteins of influenza A virus H1N1. Eur J Med Chem 2015;102:477–86.
[46] Blair W, Cox C. Current landscape of antiviral drug discovery. F1000Research 2016:5.
[47] Fani M, Teimoori A, Ghafari S. Comparison of the COVID-2019 (SARS-CoV-2) pathogenesis with SARS-CoV and MERS-CoV infections. Future Virol 2020;15:317–23.
[48] Patil P, Agrawal M, Almelkar S, Jeengar MK, More A, Alagarasu K, et al. In vitro and in vivo studies reveal α-Mangostin, a xanthonoid from Garcinia mangostana, as a promising natural antiviral compound against chikungunya virus. Virol J 2021;18:1–12.
[49] Wan YH, Wu WY, Guo SX, He SJ, Tang XD, Wu XY, et al. [1, 2, 4] Triazolo [1, 5-a] pyrimidine derivative (Mol-5) is a new NS5-RdRp inhibitor of DENV2 proliferation and DENV2-induced inflammation. Acta Pharmacol Sin 2020;41:706–18.
[50] Yuan J, Yu J, Huang Y, He Z, Luo J, Wu Y, et al. Antibiotic fidaxomicin is an RdRp inhibitor as a potential new therapeutic agent against Zika virus. BMC Med 2020;18:1–16.
[51] Zhanel GG, Walkty AJ, Karlowsky JA. Fidaxomicin: a novel agent for the treatment of Clostridium difficile infection. Can J Infect Dis Med Microbiol 2015;26:305–12.
[52] C Lee, TJ Louie, K Weiss, L Valiquette, M Gerson, W Arnott, SL Gorbach, Fidaxomicin versus vancomycin in the treatment of Clostridium difficile infection: Canadian outcomes. Canad J Infect Diseases Med Microbiol; 2016.
[53] Fu L, Ye F, Feng Y, Yu F, Wang Q, Wu Y, et al. Both Boceprevir and GC376 efficaciously inhibit SARS-CoV-2 by targeting its main protease. Nat Commun 2020;11:1–8.
[54] Vourvahis M, Davis J, Wang R, Layton G, Choo HW, Chong CL, et al. Effect of rifampin and rifabutin on the pharmacokinetics of lersivirine and effect of lersivirine on the pharmacokinetics of rifabutin and 25-O-desacetyl-rifabutin in healthy subjects. Antimicrob Agents Chemother 2012;56:4303–9.
[55] Khamitov RA, Sla L, Shchukina VN, Borisevich SV, Maksimov VA, Shuster AM. Antiviral activity of arbidol and its derivatives against the pathogen of severe acute respiratory syndrome in the cell cultures. Vopr Virusol 2008;53:9–13.
[56] Kumar SP, Kapopara RG, Patni MI, Pandya HA, Jasrai YT, Patel SK. Exploring the polymerase activity of chikungunya viral non structural protein 4 (nsP4) using molecular modeling, epharmacophore and docking studies. Int J Pharm Life Sci 2012:3.
[57] Mei M, Tan X. Current strategies of antiviral drug discovery for COVID-19. Front Mol Biosci 2021;8:310.
[58] Koulgi S, Jani V, Uppuladinne VNM, Sonavane U, Joshi R. Natural plant products as potential inhibitors of RNA dependent RNA polymerase of severe acute respiratory syndrome coronavirus-2. PLoS One 2021;16:e0251801.
[59] Yin W, Mao C, Luan X, Shen DD, Shen Q, Su H, et al. Structural basis for inhibition of the RNA-dependent RNA polymerase from SARS-CoV-2 by remdesivir. Science 2020;368:1499–504.
[60] Ghazwani MY, Bakheit AH, Hakami AR, Alkahtani HM, Almehizia AA. Virtual screening and molecular docking studies for discovery of potential RNA-dependent RNA polymerase inhibitors. Crystals 2021;11:471.
[61] Srivastava M, Mittal L, Kumari A, Asthana S. Molecular dynamics simulations reveal the interaction fingerprint of remdesivir triphosphate pivotal in allosteric regulation of SARS-CoV-2 RdRp. Front Mol Biosci 2021:8.
[62] Elfiky AA, Mahran HA, Ibrahim IM, Ibrahim MN, Elshemey WM. Molecular dynamics simulations and MM-GBSA reveal novel guanosine derivatives against SARS-CoV-2 RNA dependent RNA polymerase. RSC Adv 2022;12:2741–50.
[63] Kushwaha PP, Singh AK, Bansal T, Yadav A, Prajapati KS, Shuaib M, et al. Identification of natural inhibitors against SARS-CoV-2 drugable targets using molecular docking, molecular dynamics simulation, and MM-PBSA approach. Front Cell Infect Microbiol 2021:11.
[64] Gordon DE, Jang GM, Bouhaddou M, Xu J, Obernier K, White KM, et al. A SARS-Cov-2 protein interaction map reveals targets for drug repurposing. Nature 2020;2020(583):459–68. https://doi.org/10.1038/s41586-020-2286-9
[65] Silva Arouche TD, Reis AF, Martins AY, S Costa JF, Carvalho Junior RN, Neto JC. Interactions between remdesivir, ribavirin, favipiravir, Galidesivir, hydroxychloroquine and chloroquine with fragment molecular of the COVID-19 main protease with inhibitor N3 complex (PDB ID: 6LU7) using molecular docking (A.M.). J Nanosci Nanotechnol 2020;20:7311–23.
[66] Costanzo M, De Giglio MA, Roviello GN. SARS-CoV-2: recent reports on antiviral therapies based on lopinavir/ritonavir, darunavir/umifenovir, hydroxychloroquine, remdesivir, favipiravir and other drugs for the treatment of the new coronavirus. Curr Med Chem 2020;27:4536–41.
[67] Ahmad Jamshaid, Ikram Saima, Ahmad Fawad, Rehman Irshad Ur, Mushtaq Maryam. SARS-CoV-2 RNA Dependent RNA polymerase (RdRp)–A drug repurposing study. Heliyon 2020;6:e04502.
[68] Kullappan M, Mary U, Ambrose JM, Veeraraghavan VP, Surapaneni KM. Elucidating the role of N440K mutation in SARS-CoV-2 spike–ACE-2 binding affinity and COVID-19 severity by virtual screening, molecular docking and dynamics approach. J Biomol Struct Dyn 2021;8:1–8.